EFFECT OF RADIATION REABSORPTION ON THERMAL CHARACTERISTICS OF ELECTRIC ARCS IN AN AIR FLOW

L. N. Panasenko and V. G. Sevast'yanenko

UDC 537.523.5

The thermal characteristics of electrical arcs calculated with assumption of volume scintillation and in the presence of radiation reabsorption are compared. It is shown that consideration of radiation reabsorption significantly decreases the axial temperature and the thermal flux to the plasmotron wall.

One of the most important problems in calculating the characteristics of electrical arcs is the development and justification of suitable engineering methods for determining the divergence of radiant flux from a plasma of complex configuration with consideration of reabsorption of radiation. Problems of this type have been solved previously in a simplified formulation for arcs in argon and hydrogen [1, 2].

In the present study a new method of calculating radiant transfer [3, 4] will be used to calculate an arc in an air flow.

The system of integrodifferential equations describing an electrical arc [5] is nonlinear, and the successive approximation method must be used for numerical solution. Such a solution of a nonlinear system of equations is in itself a complex problem. Special difficulty arises in the case where the radiation is not considered in the optically thin layer approximation, as is done in calculating electric arc characteristics, but radiation transport is considered in the real spectrum with consideration of self-absorption. Then the divergence of the radiant flux $\nabla\vec{q}$, appearing in the equation for conservation of energy, and the radiant flux $\vec{q}$ itself are integrals over volume, i.e., their values at a calculation point depend on the temperature distribution (and pressure distribution if the problem is being solved for $p \neq \text{const}$) over the entire volume. Direct integration over the entire spectrum during solution of the gasdynamic problem requires large expenditures of computer time, since the electric arc plasma has a complex spectrum determined by the large number of elementary photoprocesses occurring. Consideration of radiant transfer in even one line is complex, because the absorption coefficient varies over several orders of magnitude within a narrow frequency interval. Therefore, in calculating $\nabla\vec{q}$ and $\vec{q}$ it is desirable to perform integration over frequency before solution of the gasdynamic portion of the problem. One of the simplest and most reliable methods of this type is the method of partial characteristics [3, 4]. This method permits engineering calculations of $\nabla\vec{q}$ and $\vec{q}$ for any configuration of the volume containing the radiating plasma.

We can explain the essence of the method briefly as follows. The radiant intensity $I_\nu(X)$ is the solution of the radiation transfer equation $\vec{\Omega}\nabla I_\nu = k'_\nu(I^0_\nu - I_\nu)$. Integrating along a ray $[L_b, X]$ and over frequency, we obtain at point X the value of the radiant intensity in the direction $\vec{\Omega}$ $I(X, \vec{\Omega})$ and the directional divergence $\nabla I(X, \vec{\Omega})$:

$$I(X, \vec{\Omega}) = \int_0^\infty \int_{L_b}^{X} I^0_\nu(\xi)\, k'_\nu(\xi) \exp\left(-\int_\xi^X k'_\nu(\eta)\, d\eta\right) d\xi d\nu, \tag{1}$$

$$\nabla I(X, \vec{\Omega}) = 2\int_0^\infty I^0_\nu(X)\, k'_\nu(X)\, d\nu - \int_0^\infty k'_\nu(X) \int_{L_b}^{X} I^0_\nu(\xi)\, k'_\nu(\xi) \exp\left(-\int_\xi^X k'_\nu(\eta)\, d\eta\right) d\xi d\nu. \tag{2}$$

A. V. Lykov Institute of Heat and Mass Transfer, Academy of Sciences of the Belorussian SSR, Minsk. Translated from Inzhenerno-Fizicheskii Zhurnal, Vol. 48, No. 2, pp. 279-284, February, 1985. Original article submitted November 11, 1983.

0022-0841/85/4802-0205$09.50

As was shown in [3], the absorption capability of a ray depends weakly on the concrete form of the absorption coefficient distribution $k'_\nu(\eta)$ and is determined by the integral along the ray $\int k'_\nu(\eta)d\eta$. Consequently, if we use some model temperature and pressure distributions on the ray we can integrate Eqs. (1) and (2) over frequency beforehand (before solving the gasdynamic portion of the problem). For these distributions we may use linear, bilinear, quadratic, and other splines. Depending on the temperature and pressure of the calculation point T_X and p_X, the temperature and pressure of the source T_ξ and p_ξ and the length of the segment x on which absorption occurs, tables are constructed for the partial intensity

$$\Delta I(\xi,\ X) = \int_0^\infty I^0_\nu(\xi)\, k'_\nu(\xi) \exp\left(-\int_\xi^X k'_\nu(\eta)\, d\eta\right) d\nu, \tag{3}$$

the source

$$S_{om}(X) \Big|_X^{L_b} = \int_0^\infty I^0_\nu(X)\, k'_\nu(X) \exp\left(-\int_X^{L_b} k'_\nu(\eta)\, d\eta\right) d\nu, \tag{4}$$

and the partial loss

$$\Delta S_{im}(\xi,\ X) = \int_0^\infty [I^0_\nu(\xi) - I^0_\nu(X)]\, k'_\nu(\xi)\, k'_\nu(X) \exp\left(-\int_\xi^X k'_\nu(\eta)\, d\eta\right) d\nu. \tag{5}$$

It is evident that to the accuracy of notation the source S_{om} coincides with the partial intensity ΔI. It should be noted that construction of the tables is the most cumbersome part of the problem. Once tables are prepared, use of the partial characteristics method is simple. In the present study tables published in [6] are used. Using the quantities $\Delta I(\xi, X)$, $S_{om}(X)$, and $\Delta S_{im}(\xi, X)$ the intensity $I(X, \vec{\Omega})$ and the directional divergence of the radiation $\nabla I(X, \vec{\Omega})$ are calculated:

$$I(X, \vec{\Omega}) = \int_{L_b}^X \Delta I(\xi,\ X)\, d\xi, \tag{6}$$

$$\nabla I(X, \vec{\Omega}) = S_{om}(X) \Big|_X^{L_b} - \int_{L_b}^X \Delta S_{im}(\xi,\ X)\, d\xi. \tag{7}$$

Calculations with Eqs. (6) and (7) assume that the real (i.e., those obtained from solution of the gasdynamic problem) temperature and pressure distributions on the ray $[L_b, X)$ are approximated by, for example, linear splines, and corresponding values are chosen from the partial characteristic tables for the quantities $\Delta I(\xi,\ X) = \Delta I(T_\xi,\ p_\xi,\ T_X,\ p_X,\ x)$, $S_{om}(X) \Big|_X^{L_b} = S_{om}(T_X,\ p_X,\ T_\xi,\ p_\xi,\ x_b)$ and $\Delta S_{im}(\xi,\ X) = \Delta S_{im}(T_\xi,\ p_\xi,\ T_X,\ p_X,\ x)$, where $x = |\xi - X|$, $x_b = |L_b - X|$. The point ξ traverses the entire ray from L_b to X, and the corresponding displacements $\Delta I(\xi, X)$ and $\Delta S_{im}(\xi, X)$ are summed according to Eqs. (6) and (7). To obtain values of the radiant flux and its divergence, integration over angles is performed:

$$\vec{q}(X) = \int_{(4\pi)} I(X, \vec{\Omega})\, \vec{\Omega} d\vec{\Omega}, \tag{8}$$

$$\nabla\vec{q}(X) = \int_{(4\pi)} \nabla I(X, \vec{\Omega})\, d\vec{\Omega}. \tag{9}$$

To calculate the thermal characteristics of an electric arc with longitudinal draft the present study will use the arc model described in [5], but with consideration of radiant transfer in the real spectrum. The calculation was carried out in two stages. Initially a system of difference equations was solved to find the temperature distribution over the entire channel with consideration of radiation in the optically thin layer approximation. The

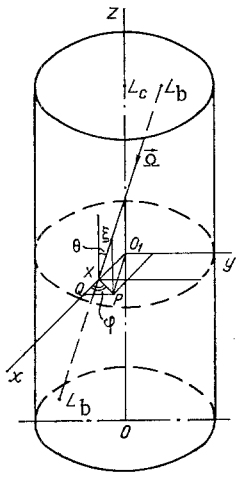

Fig. 1

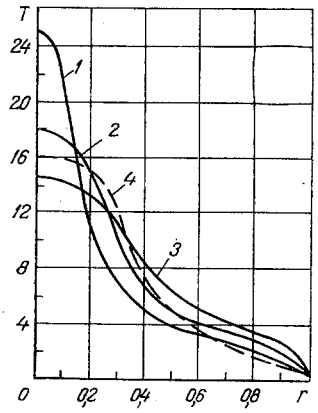

Fig. 2

Fig. 1. Geometrical model of arc used for finding radiant flux and its divergence at point X.

Fig. 2. Temperature distributions in various arc sections (I = 300 A, G = 10 g/sec, R = 1 cm, p = 0.1 MPa): 1) z = 0.7 cm; 2) 5; 3) 10; 4) 10 cm (volume radiation). T, 10^3°K; r, cm.

calculation is performed over layers in the direction of the z axis with variable step Δz. In each layer the difference equations were solved by the flow drive method. The difference system is the same used in [5]. The step in radius Δr is equal to 0.02, i.e., 50 points along the radius were used in the calculation. The step Δz varied from 10^{-5} to 0.05, and the difference equations were solved in 82 layers. Considering the symmetry of the problem, it is sufficient to solve the difference equations for half of the cylinder. In considering radiant transfer the entire arc volume is used.

In the second stage, using the temperature distribution calculated in the first stage, the partial characteristics method is used to calculate $\nabla\vec{q}$ and $\vec{q}$. For the cylindrical calculation region shown in Fig. 1, Eqs. (8) and (9) take on the form

$$q_x(X) = -\int_0^{\pi}\int_0^{2\pi}\int_X^{L_b} \Delta I(T_\xi,\ T_X,\ x)\, a\xi \cos\varphi \sin^2\theta\, d\varphi d\theta, \tag{10}$$

$$q_y(X) = -\int_0^{\pi}\int_0^{2\pi}\int_X^{L_b} \Delta I(T_\xi,\ T_X,\ x)\, d\xi \sin\varphi \sin^2\theta d\varphi d\theta, \tag{11}$$

$$q_z(X) = -\int_0^{\pi}\int_0^{2\pi}\int_X^{L_b} \Delta I(T_\xi,\ T_X,\ x)\, a\xi \cos\theta \sin\theta d\varphi d\theta, \tag{12}$$

$$\nabla\vec{q}(X) = \int_0^{\pi}\int_0^{2\pi}\left[S_{om}(T_X,\ T_\xi,\ x_b) - \int_X^{L_b} \Delta S_{im}(T_\xi,\ T_X,\ x)\, d\xi\right]\sin\theta d\varphi d\theta. \tag{13}$$

Integration over the ray in Eqs. (10)-(13) is replaced by summation, moving with a step Δx until the boundary of the calculation region is reached (Fig. 1).

The calculation was performed assuming constant pressure. The temperature distribution between the points X and ξ was approximated by linear splines. The temperature at point X was taken from the solution of the problem in the previous stage, since the point X is located at the calculated radius. The temperature T_ξ is not known before hand. In order to find this value the coordinates of the point ξ are determined, as shown in Fig. 1. The coordinates of the point X are specified in a cylindrical coordinate system with origin at point 0, at which the entire problem was solved ($\rho_x = r_i = r_{i-1} + \Delta r$, $z_x = z^j = z^{j-1} + \Delta z$). To find the coordi-

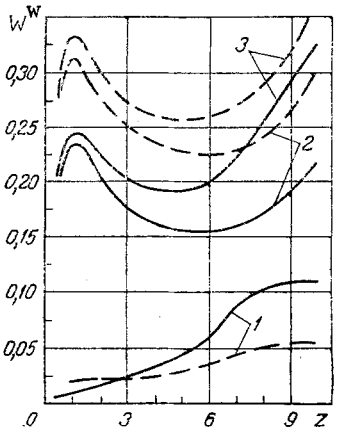

Fig. 3

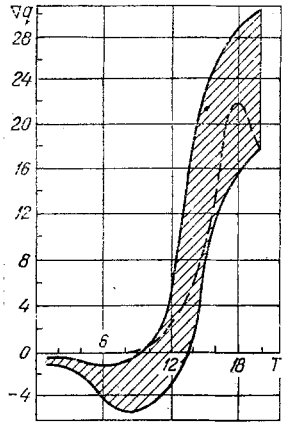

Fig. 4

Fig. 3. Distribution of thermal flux into plasmotron wall over channel length (I = 300 A, G = 5 g/sec, R = 1 cm, p = 0.1 MPa): 1) conductive flux; 2) radiation; 3) total flux; dashed curves, volume radiation approximation. W_2^W, kW/cm²; z, cm.

Fig. 4. Dependence of divergence of radiant flux on temperature. Air, p = 0.1 MPa. Δq, kW/cm³; T, 10^3°K.

nates ρ_ξ and z_ξ in this system two other coordinate systems with origin at the point X are required: a Cartesian system in which the coordinates of the point ξ are calculated, and a spherical one, in which the direction of the ray $\vec{\Omega}$ is specified by angles θ and φ (the steps Δθ and Δφ are known). The X axis of the Cartesian system is parallel to the r axis of the cylindrical system. From the triangles $\Delta X\xi P$, ΔXPQ and ΔO_1QP, we find

$$\rho_\xi = (x^2 \sin^2\theta + 2x\rho_X \sin\theta\cos\varphi + \rho_X^2)^{1/2},\ z_\xi = x\cos\theta + z_X, \tag{14}$$

where x is the distance between the points X and ξ on the ray [L_b, X). The temperature $T_\xi(\rho_\xi, z_\xi)$ is determined by interpolation from the previously calculated field T(r, z). In order to remain within the limits of the cylinder, the coordinates of each point ξ are tested for satisfaction of the conditions

$$\rho_\xi^2 \leqslant R^2,\ 0 \leqslant z_\xi \leqslant L_c, \tag{15}$$

where R and L_c are the radius and length of the channel. Knowing T_ξ, T_X, and x, by interpolation from the partial characteristic tables we find $\Delta I(T_\xi, T_X, x)$, $\Delta S_{im}(T_\xi, T_X, x)$, and $S_{om}(T_X, T_\xi, x_b)$. The latter can be found from the table of partial intensities ΔI by exchanging the places of the temperatures T_ξ and T_X. When calculating the quantity S_{om} the "source" of radiation is the point X. This method was used in each layer z of the difference system to calculate $\nabla\vec{q}$ and a new temperature distribution. Since all transfer coefficients depend on T, their determination requires iterations. Calculation on an ES-1022 computer showed that two repetitions are sufficient for convergence of the iteration process.

The model of [5], which was used for description of the arc with consideration of radiation transfer in the real spectrum, allows calculation of the following characteristics: distributions of temperature, axial velocity, specific mass flow rate, radiant flux divergence, r and z components of the radiant flux, conductive and convective heat fluxes along radius and channel length, as well as the change in electric field intensity, mean mass enthalpy, and thermal flux to the plasmotron wall along channel length.

Calculations were performed for an arc with longitudinal air draft. The current varied from 100 to 500 A, and the gas flow rate from 2 to 10 g/sec. Arc characteristics were calculated for channels with radii of 0.5 and 1 cm. The channel length in all variants was 10 cm. The dependence of thermal and electrical conductivity coefficients on temperature was taken from [7], and density and specific heat, from [8].

Consideration of radiation reabsorption in the real spectrum (Fig. 2) reduces the axial temperature in the different variants by 500-2000°K, while the plasma temperature near the wall increases by 1000°K. At the channel wall gas heating occurs mainly because of reabsorption of radiation. The role of conductive heat flow is small here (Fig. 3). Upon considering radiant transfer in the real spectrum the conductive flux into the channel wall increases,

since in this case large temperature gradients occur at the wall, while the radiant flux decreases due to reabsorption. But since the fraction of conductive thermal flux in the total thermal flux into the channel wall is much less than the fraction of radiant flux, the total flux behaves like the radiant, i.e., decreases as compared to the case of volume radiation.

The effect of reabsorption on gas heating is shown in Fig. 4. In the case of volume radiation the dependence of radiant flux divergence on temperature from [9] was used. When reabsorption of radiation is considered, as was noted above, $\nabla\vec{q}$ depends on the temperature distribution over the entire volume, and consequently, for the different calculation variants this function is expressed by different curves $\nabla\vec{q}(T)$. In Fig. 4 the range of $\nabla\vec{q}(T)$ values for all variants is hatched, the upper boundary corresponding to low current (100 A), and lower, to high current (500 A). In the temperature range 1000-10,000°K the radiant flux divergence is a negative quantity, i.e., in the equation for conservation of energy it appears as an additional heat source. In the case of volume radiation in this temperature range $\nabla\vec{q}=0$. By analyzing the position of the function $\nabla\vec{q}(T)$ for volume radiation in Fig. 4 it can be noted that use of the volume radiation approximation produces a large error, especially in calculating hot layers of the arc near the axis. At the wall use of this approximation is completely unjustifiable.

NOTATION

$\vec{\Omega}$, radiation direction unit vector; I_ν°, spectral intensity of equilibrium radiation; k_ν', absorption coefficient; ν, frequency; ξ, radiating point; X, calculation point; L_b, boundary of region with radiating gas; I, current; G, gas flow rate.

LITERATURE CITED

1. Vetlutskii et al., "Calculation of an electric arc in argon, stabilized by walls, with consideration of radiant energy transfer," Zh. Prikl. Mekh. Tekh. Fiz., No. 4, 71-78 (1965).
2. A. T. Onufriev and V. G. Sevast'yanenko, "Calculation of a cylindrical electrical arc with consideration of radiant energy transfer," Zh. Prikl. Mekh. Tekh. Fiz., No. 2, 17-22 (1968).
3. V. G. Sevast'yanenko, "Energy transfer in the real spectrum. Integration over frequency," Inzh.-Fiz. Zh., 36, No. 2, 218-229 (1979).
4. V. G. Sevast'yanenko, "Energy transfer in the real spectrum. Integration over frequency and angles," Inzh.-Fiz. Zh., 38, No. 2, 278-285 (1980).
5. A. F. Bublievskii et al., "The character of thermal flux distribution over plasmotron channel length," Izv. Akad. Nauk Beloruss. SSR. Ser. Fiz.-Energ. Nauk, No. 1, 127-133 (1981).
6. V. G. Sevast'yanenko, "Radiant heat transfer in the real spectrum," Author's Abstract of Doctoral Dissertation, Novosibirsk (1980).
7. I. A. Sokolova, "Transfer coefficients for air in the temperature range from 3000 to 25,000°K and pressures of 0.1, 1.0, 10, and 1000 atm," Zh. Prikl. Mekh. Tekh. Fiz., No. 2, 80-90 (1973).
8. A. S. Predvoditelev et al., Tables of the Thermodynamic Functions of Air [in Russian], Izd. Akad. Nauk SSSR, Moscow (1962).
9. B. Kivel, "Radiation from hot air and its effect on stagnation point heating," J. Aerospace Sci., 28, No. 2, 96-102 (1961).